Theoretical and experimental investigations on metallic acoustic lenses

Sallam, Ahmed, Meesala, Vamsi C., Shahab, Shima

Ahmed Sallam, Vamsi C. Meesala, Shima Shahab, "Theoretical and experimental investigations on metallic acoustic lenses," Proc. SPIE 11588, Active and Passive Smart Structures and Integrated Systems XV, 1158807 (22 March 2021); doi: 10.1117/12.2583141

SPIE.

Event: SPIE Smart Structures + Nondestructive Evaluation, 2021, Online Only

Theoretical and Experimental Investigations on Metallic Acoustic Lenses

Ahmed Sallam[1], Vamsi C. Meesala and Shima Shahab
Department of Mechanical Engineering, Virginia Tech, Blacksburg, VA,24060

ABSTRACT

This work introduces and investigates a metallic acoustic holographic lens to create an arbitrary acoustic pressure pattern in a target plane, using sound reflection phenomenon. The lens performs as a spatial sound modulator by introducing a relative phase shift to the reflected wavefront. The phase-shifting lens is designed using an iterative angular spectrum algorithm, and 3D-printed from powdered aluminum through direct metal laser melting. Then its capabilities to construct diffraction-limited complex pressure patterns and create multifocal areas are tested under water, numerically and experimentally. The proposed holographic lens design can drive immense improvements in applications involving medical ultrasound, ultrasonic energy transfer, and particle manipulation.

Keywords: Acoustic holograms, Metamaterial, Sound manipulation, Ultrasonics, Acoustic lenses, Phase modulation

1. INTRODUCTION

The fine spatial manipulation of sound waves is crucial for a broad range of applications such as medical ultrasound[1,2], acoustic energy transfer (AET)[3–7],non-destructive evaluation (NDE)[8,9], and particle manipulation[10,11]. As such, developments in wave manipulation techniques can drive immense improvements in current applications give rise to new transformative technologies in acoustics. Currently, acoustic manipulation is achieved mainly using active phased arrays transducers (PATs). It is an active manipulation technique where a large number of acoustic sources are driven using complex electronic circuitry. By tuning the operating phase and amplitude of these transducers complex and dynamic wavefronts can be generated. PATs enabled new technologies in acoustics such as acoustic tweezers[12], three-dimensional particle manipulation[13]. Scaling to high-resolution control requires an impractically large number of transducers with sophisticated, complex and power-consuming circuitry[14]. In addition, if the size of each transducer is comparable to the size of the wavelength of the waves they generate, the accuracy of the control over the sound field is severely limited[15]. More recently, metamaterials showed exotic properties such as wavefront transformation[16,17], and acoustic manipulation via amplitude and phase modulation[18]. However, most of these studies have been in air for a range of frequencies between 1-17 kHz. Extending the use of metamaterials for the ultrasonic range is challenging and requires advanced fabrication techniques, since metamaterials are made of arrays of sub-wavelength size unit cells[19,20].

Alternatively, the static 3D-printed spatial sound modulators (SSM), first introduced by Melde et al.[14], enabled an unprecedented level of control in the ultrasonic range. By storing the phase information in the topology of the modulator, elaborate pressure patterns can be constructed when a suitable acoustic source s used. The capabilities of this technology have been demonstrated in particle assembly[14], phase and amplitude modulation[21] and focusing of ultrasonic fields through the human skull[22]. Although these passive acoustic lenses lack the dynamic real-time control offered by PATs, efforts have been made to achieve some temporal command over the modulated sound field by using multi-frequency holograms[23], arrays of piston actuators that act as variable-length wave modulators[15] and real-time controlled microbubble arrays[24]. The majority of the work has been done on transmission holograms fabricated by 3D-printed polymers. In this context, we introduce a 3D-printed metal-based reflective holographic lens capable of constructing diffraction-limited intricate

[1] Corresponding author email address: ahmedsallam@vt.edu

Active and Passive Smart Structures and Integrated Systems XV, edited by Jae-Hung Han, Gang Wang, Shima Shahab, Proc. of SPIE Vol. 11588, 1158807 · © 2021 SPIE · CCC code: 0277-786X/21/$21 · doi: 10.1117/12.2583141

pressure patterns in desired locations in space. As shown in Fig. 1, the metallic hologram reflects an acoustic wave generated by a piezoelectric disc transducer that is located between the hologram plane and the target plane.

The thickness map of the holographic lens introduces a phase shift distribution to the reflected wavefront. The reflected wave then propagates downstream with the phase distribution required to project the pressure pattern at the desired target plane. Similar to transmission holograms, this monolithic hologram can be fabricated using available additive manufacturing techniques, its suitable for high-frequency applications up to the MHz range and can work underwater.

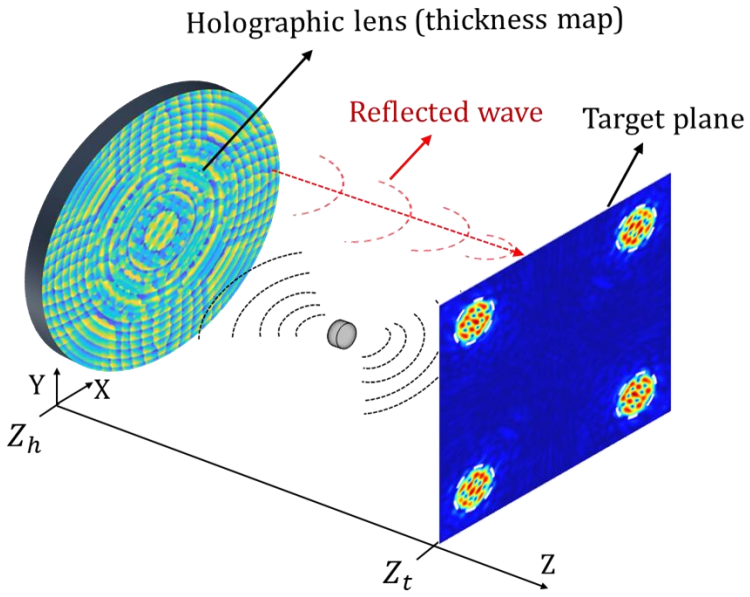

Figure 1. Schematic depiction of the reflective holographic lens. The lens reflects the incoming acoustic wave from the cylindrical acoustic transmitter and modulates its phase to construct a desired amplitude pressure pattern at the target plane.

2. THEORY

To compute the thickness map of the holographic lens, we must first compute the complex pressure phase distribution at the hologram plane $Z = Z_h$ that produces the desired pressure pattern at the target plane $Z = Z_t$ as shown in Fig. 1. The phase information is then translated to the thickness map, which can then be fabricated using direct metal laser melting (DMLM). In this work, we use the iterative angular spectrum algorithm (IASA) [14,25]. Figure 2 summarizes the workflow of the algorithm. It starts by imposing two boundary conditions, the reflected pressure amplitude at the hologram plane shown in Fig. 2(a) and the desired amplitude pattern at the target plane shown in Fig. 2(b). The phase is left to vary freely with no constraints or limitations imposed on it. Multiple iterations of front and back propagations between the two planes are then carried out until a phase map that corresponds to a satisfactory pressure pattern is achieved.

Similar to the procedure followed by Melde et al.[14], the pressure distribution is predicted at the target plane by forward-propagating it using

$$p(x,y,Z_t) = IFT[FT[p(x,y,Z_h)]e^{iZ\sqrt{(k^2-k_x^2-k_y^2)}} \quad (1)$$

and similarly, for back-propagation

$$p(x,y,Z_h) = IFT[FT[p(x,y,Z_t)]e^{-iZ\sqrt{(k^2-k_x^2-k_y^2)}} \quad (2)$$

where FT and IFT are Fourier transform and it's inverse respectively, k is the wavenumber, and $p(x, y, Z_h)$ and $p(x, y, Z_t)$ are the complex pressure distributions respectively at the hologram and target planes.

The obtained phase, shown in Fig. 2(c), is then transformed to the thickness map of the lens using $t(x, y) = t_0 + \Delta\phi(x, y)/2k_w$ where $t(x, y)$ is the thickness map, t_0 is the initial thickness of the flat lens, k_w is the wavenumber in water, and $\Delta\phi(x, y)$ is the phase change map. The phase change map represents the phase shift that must be introduced to the initial phase distribution of the reflected pressure to achieve the theoretical pressure distribution shown in Fig. 2(d).

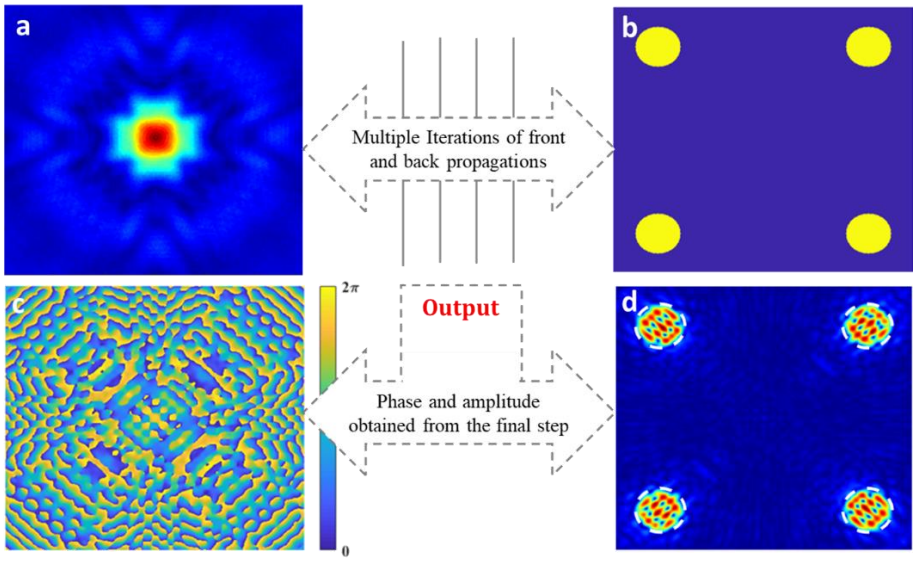

Figure 2. The scheme of generating phase distribution using IASA. a) Reflected pressure amplitude at the hologram plane. b) Desired amplitude map at the target plane. c) Obtained phase distribution at the hologram plane. d) Theoretical prediction of the pressure amplitude at the target plane.

As mentioned above, the first step in designing the lens is determining the reflected complex pressure at the hologram plane. Due to the difficulty of obtaining the reflected pressure experimentally, the lens and the transmitter were simulated underwater using the FEM software COMSOL Multiphysics 5.4. The analysis was carried out using the Acoustic-Piezoelectric interaction, Frequency Domain Multiphysics interface. The reflected pressure was calculated using $p_{ref} = p_{tot} - p_{inc}$, where p_{inc} and p_{tot} are the incident pressure and total pressure at the hologram plane, respectively.

3. EXPERIMENTAL SETUP, RESULTS AND DISCUSSION

To validate the proposed approach for designing the reflective lens, we performed two sets of experiments under water. A metallic holographic lens Fig. 3 (a) with the thickness map shown in Fig. 3 (c) was fabricated with powdered aluminum (AlSi10Mg) by 3D printing it (Stratasys) using the direct metal laser melting (DMLM) technique with a theoretical printing resolution of 20 µm in the z-direction. The lens is disc-shaped with a diameter of 9 cm and an average thickness of 1 cm, it is designed to construct the four focal areas pressure pattern in Fig. 2 (b) in a target plane that is 7 cm away from the lens in the z-direction at an operating frequency of 780 kHz. The lens was illuminated by a piezoelectric transducer, it is disc-shaped and has a 9 mm diameter and a 3mm thickness, it was placed 3.5 cm away from

the lens and it was excited by a sinusoidal pulse signal with an amplitude of 103 V provided by an arbitrary function generator (Keysight 33500B) and an amplifier (Electronics & Innovation A075). The lens and the transducer were mounted under water in a tank with walls partially covered with acoustic absorbing sheets. To map the pressure field, a 3D positioning system was responsible for moving a needle hydrophone to a user-defined set of measuring points on the target plane as shown in Fig. 3 (b). To avoid aliasing the signal was sampled with a spatial resolution of $\lambda/2$. The signal from the hydrophone was then fed to an oscilloscope (Tektronix TBS2104) and then post-processed with MATLAB.

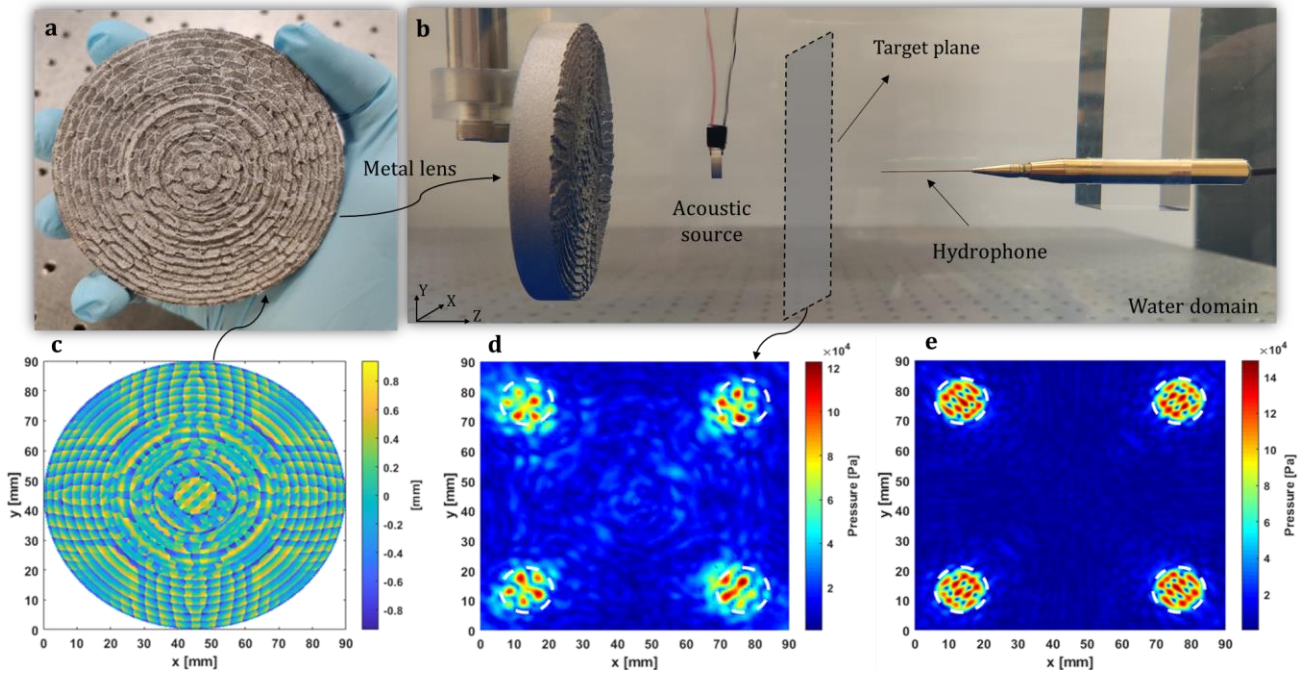

Figure 3. (a) Printed holographic lens, (b) the experimental setup with the printed lens, piezoelectric disc acoustic source, (c) the lens thickness map. (d) Experimentally measured pressure amplitude distribution at the target plane. (e) Theoretical pressure amplitude distribution at the target plane.

In the first set of experiments, we considered a pattern with four uniform focal areas (circles with a diameter of 1.5 cm as shown in Fig. 2 (b)) at the target plane to demonstrate the lens capability for focusing the acoustic energy in desired focal areas. The experimentally obtained pressure distribution and the theoretical prediction of the pressure pattern are presented in Fig 3(d) and Fig. 3(e), respectively, which show a good agreement. We then determine the focusing efficiency to assess the obtained results both qualitatively and quantitively. The focusing efficiency is defined as $\eta = P_A/P_{total}$, where P_{total} is the total acoustic power of the whole field and P_A is the acoustic power over the focal areas[26]. The theoretical efficiency is calculated to be 61%, while the experimental efficiency is 34%. The results also reveal that the experimental pattern did not align perfectly with the desired pattern. These errors can be attributed to misalignments, uncertainties in the hydrophone sensitivity, fabrication imperfections, and material inhomogeneities.

In the second set of experiments, we demonstrate the lens capabilities for elaborate pressure patterning by considering the flower-shaped pressure pattern shown in Fig. 4(a). The corresponding phase distribution and thickness map generated using the proposed approach are presented respectively in Fig. 4(b) and Fig. 4(c). The experimentally measured pressure amplitude distribution at the target plane is shown in Fig. 4(d). By comparing it with the theoretical prediction shown in Fig. 4(e), we note that a good agreement is achieved in the general pattern of the target and that the locations of high-pressure points in the experiment match closely to those of the theoretical prediction. The obtained results also show that

the experimental pressure pattern is not as clean as the theoretical prediction and that there is a slight disagreement in the amplitude of pressure. We attribute this inconsistency to the reasons mentioned above.

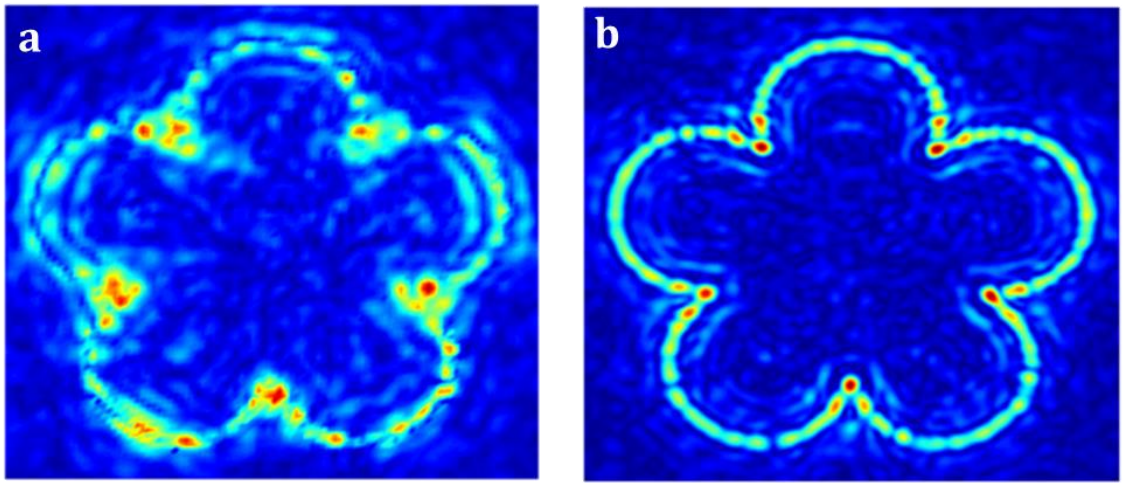

Figure 4. (a) Experimentally measured pressure amplitude distribution at the target plane. (b) Predicted theoretical pressure amplitude distribution at the target plane.

4. CONCLUSIONS

We introduced a 3D-printed metallic reflective lens for the intricate manipulation of ultrasonic acoustic waves under water. We designed, fabricated, and experimentally tested the capabilities of the proposed lens for elaborate pressure pattering and amplitude focusing. Such a lens can manipulate sound fields with high resolution without the need for costly and complex hardware. We envision the proposed concept has the potential to extend the realm of critical applications that employ acoustic holography. Notably, the pressure patterning is of interest for particle manipulation as well as medical ultrasound. Furthermore, the ability to focus sound on multifocal areas with a single transmitter is desirable for wirelessly recharging and communicating with sensor networks using acoustic energy transfer (AET). Additionally, integrating reflective and transmission holograms can increase the power transfer efficiency in AET systems by utilizing the otherwise unexploited acoustic energy and enable the control of both phase and amplitude[21] in acoustic holography.

ACKNOWLEDGMENTS

This work is supported by NSF grants Award No. ECCS - 1711139 and IIP 1738689 (PhaseII IUCRC VirginiaTech: Center for Energy Harvesting Materials and Systems), which are gratefully acknowledged.

REFERENCES

[1] Miller, D., Smith, N., Bailey, M., Czarnota, G., Hynynen, K. and Makin, I., "Overview of Therapeutic Ultrasound Applications and Safety Considerations," J. Ultrasound Med. Off. J. Am. Inst. Ultrasound Med. **31**(4), 623–634 (2012).

[2] Wells, P. N. T., "Ultrasound imaging," Phys. Med. Biol. **51**(13), R83–R98 (2006).

[3] Bakhtiari-Nejad, M., Elnahhas, A., Hajj, M. R. and Shahab, S., "Acoustic holograms in contactless ultrasonic power transfer systems: Modeling and experiment," J. Appl. Phys. **124**(24), 244901 (2018).
[4] Bhargava, A., Meesala, V. C., Hajj, M. R. and Shahab, S., "Nonlinear effects in high-intensity focused ultrasound power transfer systems," Appl. Phys. Lett. **117**(6), 064101 (2020).
[5] Shahab, S., Gray, M. and Erturk, A., "Ultrasonic power transfer from a spherical acoustic wave source to a free-free piezoelectric receiver: Modeling and experiment," J. Appl. Phys. **117**(10), 104903 (2015).
[6] Meesala, V. C., Hajj, M. R. and Shahab, S., "Analysis and prediction of shock formation in acoustic energy transfer systems," J. Appl. Phys. **128**(23), 234902 (2020).
[7] Meesala, V. C., Hajj, M. R. and Shahab, S., "Modeling and identification of electro-elastic nonlinearities in ultrasonic power transfer systems," Nonlinear Dyn. **99**(1), 249–268 (2020).
[8] Gholizadeh, S., "A review of non-destructive testing methods of composite materials," Procedia Struct. Integr. **1**, 50–57 (2016).
[9] Grosse, C. U. and Ohtsu, M., [Acoustic Emission Testing], Springer Science & Business Media (2008).
[10] Marzo, A., Ghobrial, A., Cox, L., Caleap, M., Croxford, A. and Drinkwater, B. W., "Realization of compact tractor beams using acoustic delay-lines," Appl. Phys. Lett. **110**(1), 014102 (2017).
[11] Marzo, A., Caleap, M. and Drinkwater, B. W., "Acoustic Virtual Vortices with Tunable Orbital Angular Momentum for Trapping of Mie Particles," Phys. Rev. Lett. **120**(4), 044301 (2018).
[12] Marzo, A., Seah, S. A., Drinkwater, B. W., Sahoo, D. R., Long, B. and Subramanian, S., "Holographic acoustic elements for manipulation of levitated objects," 1, Nat. Commun. **6**(1), 8661 (2015).
[13] Prisbrey, M. and Raeymaekers, B., "Ultrasound Noncontact Particle Manipulation of Three-dimensional Dynamic User-specified Patterns of Particles in Air," Phys. Rev. Appl. **10**(3), 034066 (2018).
[14] Melde, K., Mark, A. G., Qiu, T. and Fischer, P., "Holograms for acoustics," 7621, Nature **537**(7621), 518–522 (2016).
[15] Prat-Camps, J., Christopoulos, G., Hardwick, J. and Subramanian, S., "A Manually Reconfigurable Reflective Spatial Sound Modulator for Ultrasonic Waves in Air," Adv. Mater. Technol. **5**(8), 2000041 (2020).
[16] Li, J., Song, A. and Cummer, S. A., "Bianisotropic Acoustic Metasurface for Surface-Wave-Enhanced Wavefront Transformation," Phys. Rev. Appl. **14**(4), 044012 (2020).
[17] Chiang, Y. K., Oberst, S., Melnikov, A., Quan, L., Marburg, S., Alù, A. and Powell, D. A., "Reconfigurable Acoustic Metagrating for High-Efficiency Anomalous Reflection," Phys. Rev. Appl. **13**(6), 064067 (2020).
[18] Zhu, Y., Hu, J., Fan, X., Yang, J., Liang, B., Zhu, X. and Cheng, J., "Fine manipulation of sound via lossy metamaterials with independent and arbitrary reflection amplitude and phase," 1, Nat. Commun. **9**(1), 1632 (2018).
[19] Ma, G. and Sheng, P., "Acoustic metamaterials: From local resonances to broad horizons," Sci. Adv. **2**(2), e1501595 (2016).
[20] "Active times for acoustic metamaterials | Elsevier Enhanced Reader.", <https://reader.elsevier.com/reader/sd/pii/S2405428318300649?token=210F1426C624B9BF91ED3D9593938A454B98075719EE7D46578A1DB93F6D69F557A38BA37F2F2444726C4A3EE7B1615A> (18 January 2021).
[21] Brown, M. D., "Phase and amplitude modulation with acoustic holograms," Appl. Phys. Lett. **115**(5), 053701 (2019).
[22] Jiménez-Gambín, S., Jiménez, N., Benlloch, J. M. and Camarena, F., "Holograms to Focus Arbitrary Ultrasonic Fields through the Skull," Phys. Rev. Appl. **12**(1), 014016 (2019).
[23] Brown, M. D., Cox, B. T. and Treeby, B. E., "Design of multi-frequency acoustic kinoforms," Appl. Phys. Lett. **111**(24), 244101 (2017).
[24] Ma, Z., Melde, K., Athanassiadis, A. G., Schau, M., Richter, H., Qiu, T. and Fischer, P., "Spatial ultrasound modulation by digitally controlling microbubble arrays," Nat. Commun. **11**(1), 4537 (2020).
[25] Mellin, S. D. and Nordin, G. P., "Limits of scalar diffraction theory and an iterative angular spectrum algorithm for finite aperture diffractive optical element design," Opt. Express **8**(13), 705–722 (2001).
[26] Tarrazó-Serrano, D., Pérez-López, S., Candelas, P., Uris, A. and Rubio, C., "Acoustic Focusing Enhancement In Fresnel Zone Plate Lenses," 1, Sci. Rep. **9**(1), 7067 (2019).